Optimal Design and Numerical Analysis of Soil Slope Reinforcement by a New Developed Polymer Micro Anti-slide Pile

Yuke Wang (ykewang@163.com)
Zhengzhou University https://orcid.org/0000-0003-1849-4857
Musen Han
Zhengzhou University
Xiang Yu
Zhengzhou University
Chengchao Guo
Zhengzhou University
Jinggan Shao
Henan jiaoyuan engineering technology Co., Ltd

Research Article

Keywords: polyurethane polymer, embedded depth, pile position, mises stress, multi factor comprehensive evaluation method

Posted Date: June 2nd, 2021

DOI: https://doi.org/10.21203/rs.3.rs-503680/v1

Optimal design and numerical analysis of soil slope reinforcement by a new developed polymer micro anti-slide pile

Yuke Wang[1,2,3], Musen Han[1,2,3], Xiang Yu[1,2,3*], Chengchao Guo[1,2,3], Jinggan Shao[4]

(1. College of Water Conservancy Engineering, Zhengzhou University,. Zhengzhou, 450001, China; 2. National Local Joint Engineering Laboratory of Major Infrastructure Testing and Rehabilitation Technology, Zhengzhou, 450001, China; 3. Collaborative Innovation Center of Water Conservancy and Transportation Infrastructure Safety, Henan Province, Zhengzhou 450001, China; 4. Henan Jiaoyuan Engineering Technology Co., Ltd , Zhengzhou, 450001, China)

Abstract: As a new material, polyurethane polymer has been widely used in engineering in recent years due to the excellent engineering mechanical properties. Based on the characteristics of this material, a multi pipe grouting micro anti-slide pile is proposed, which is formed by using polymer slurry as grouting material. Compared with traditional anti-slide pile, the polymer micro pile has the advantages of strong applicability, no water reaction, small disturbance, fast construction, economy and durability. As a flexible retaining structure, polymer micro-piles can strengthen the slope by cooperating with the forces. However, there is no report on the reinforcement of slope by polymer micro piles at present. In this paper, a three-dimensional multi row polymer micro piles model for slope reinforcement considering different embedded depth and pile location is established. Safety factor, thrust force of landslide behind pile, length of pile and mises stress are taken as four factors to evaluate reinforcement effect, the optimal reliability of polymer micro anti-slide pile for slope reinforcement is evaluated by giving different weight values to each factor through multi factor comprehensive evaluation method. The safety factor of slope (F_s), landslide thrust behind pile and mises stress of pile are analyzed under different embedded depth (l_e) and pile position (p_x). The results show that the best embedded depth is about1/8-1/12 of the horizontal length of the landslide behind the pile when multi row polymer micro piles are used to reinforce the slope; the optimum position of pile arrangement is 0.55-0.65 times the slope length from the top of the slope.

Key words: polyurethane polymer; embedded depth; pile position; mises stress; multi factor comprehensive evaluation method.

1 Introduction

With the development of people's continuous exploration, new alloys, ceramics, glass, organic materials and other synthetic materials, various composite materials occupy an increasingly important position in engineering. Since the 1960s, the research and application of chemical grouting materials, such as polyurethane polymer, have been widely valued in engineering construction. As a new type of grouting material for foundation reinforcement, polymer has unique advantages compared with other engineering materials such as concrete: 1) early-high-strength, convenient construction; 2) self-inflating; 3) light weight; 4) elastic layer, good crack resistance; 5) good durability. In recent years, it has been widely used in many industries, showing a huge application space and development prospects. For polymer materials, domestic and foreign scholars have carried out a preliminary discussion: the experimental study on the compressive strength of polymer materials was carried out in Padua University of Italy

(2004), and the quadratic relationship between the compressive strength and the density of polymer was given. (Naudts 2003) reviewed the development history of polyurethane materials, and introduced non-aqueous reactive polyurethane materials. (Wang et al. 2014) made a comprehensive study on the chemical characteristics, compressive strength and tensile strength of polymer materials, and explored and analyzed the diffusion law of polymer in soil and the bonding characteristics with silt, the diffusion mechanism of polymer grouting was numerically simulated by (Hao et al. 2018).

The proportion of landslide disasters is much higher than other geological disasters in each year. To control landslide disasters is a subject that engineers have been studying all the time. (He et al. 2020; Liu et al. 2020) has studied the effective pile reinforcement through experiment, which has changed the development of reservoir landslide and made the whole sliding surface not reach the critical state. (Ausilio et al. 2001) used limit analysis method to analyze the stability of the slope, and derived the expression of the force required to increase the safety factor to the expected value. (Gao et al. 2015) found that when the slope is reinforced by row piles with small pile spacing, the role of pile groups is of great significance to the safety evaluation of the slope. This method is more suitable for stability evaluation of slope reinforced by pile foundation and design of stability layer of unstable slope. (Xue et al. 2018) carried out finite element analysis on pre-reinforced side slope of row piles at different excavation stages and found that pre-reinforced piles are very important to stability of side slope. Meanwhile, the influence of pile position should be carefully considered in design. (Tan et al. 2018) proposed a strategy, called Local Safety Zoning (LSP), for precisely determining the optimal pile position under the stepped structure. This method cuts the landslide mass into blocks, calculates the local safety factor of each block, and identifies the optimal pile position. The LSP method does not consider the influence of other factors but the effect of reinforcement. (Tang et al. 2018) studied the influence of pile length, position of pile sheet, pile stiffness and soil properties on the performance of piles. (Li et al. 2019; Mao et al. 2019) found that the deformation patterns of adjacent piles in pile groups are different, resulting in different degrees of axial forces and bending moments. Piles in the shear zone will separate and pile groups will be destroyed with the increase of fault displacement. (Tang et al. 2014) found that the maximum soil pressure exerted by anti-sliding piles occurs in the middle and upper part of the sliding mass. The distribution of soil pressure has complex changing rules during deformation. These influences must be considered in the analysis and design of anti-sliding piles. (Won et al. 2005; Cai and Ugai 2000) used FLAC 3D to coupling analysis of anti-slide pile in slope. According to the shear strength reduction technology, he calculated the safety factor of the slope reinforced by piles. It was found that the safety factor was significantly higher when the pile was located in the middle of the slope.

Based on the analysis above, polymer materials are mostly used for foundation reinforcement and dam seepage control by grouting. However, there are few studies on the micro anti-slide pile formed by using polyurethane polymer as grouting material. The design scheme and structural stress law of the slope reinforced by polymer micro pile are not clear, and the related stability research is almost blank. In this paper, combined with the

research of (Zhao et al. 2017; Disfani et al. 2018; Surjandari et al. 2017; Kourkoulis et al. 2011), and through the method of numerical analysis and multi factor comprehensive evaluation, the calculation model of polymer micro anti-slide pile is established, and the design scheme of polymer micro pile reinforcement slope is verified and evaluated.

2 Calculation model of polymer micro anti-slide pile

Different from cement mortar, the polymer mixture with specific proportion has good fluidity, expansibility, fast forming speed, high strength and long service life after forming. Polymer micro piles are made of polymer slurry by pressure grouting. In the process of construction, the high polymer slurry is injected into the predetermined area by grouting machine to form pile, which makes full use of the good fluidity and fast forming characteristics of high polymer slurry to form a structure similar to anchor solid around the pile. In the finite element analysis software, it is simplified as a circular solid are shown in Fig.1. According to the special diffusion effect of polymer slurry (Wang et al. 2014; Hao et al. 2018), the finite element strength reduction method is used to analyze the stability of slope reinforced by polymer micro anti-slide pile. The anti-slide pile model with diameter D=30 cm and the high polymer soil ring pile model with thickness D=5 cm around the pile are established; the slope gradient is i=0.4, the slope height is 20 m, the slope length is 50 m, the ground to underground 2 m is silty clay, below 2 m is granite. In order to study the reinforcement effect of pile group, the pile row number is 5, the pile spacing is 3D = 0.9 m, the pile is arranged in quincunx shape, and the pile section is circular. The ideal elastic-plastic model obeying Mohr Coulomb failure criterion is adopted for slope soil. The interaction mode between pile and soil is normal contact, the contact property is "hard contact", and the friction coefficient is 0.46. Combined with the horizontal displacement at the foot of the slope and the vertical displacement at the top of the slope, forming plastic penetration zone as the instability criterion of the slope. The initial stress field is considered as gravity field, and all models adopt unified boundary conditions. The horizontal displacement of the left and right sides of the slope is constrained in Z direction, the front and back sides are constrained in X direction, and the bottom side is fully constrained in X, Y and Z directions, the three-dimensional stress c3d8 attribute is used for mesh generation, and the mesh generation is shown in Fig.1. The finite element software is used to calculate, and the stability factor is F_s=1.205 when there is no support to reinforce the slope. The relevant parameters of the calculation model are shown in Table 1, and the schematic diagram of the slope model strengthened by polymer micro piles is shown in Fig.2.

3 Influence of design parameters of slope reinforced by anti-slide pile

In the process of slope reinforcement design, geotechnical engineers should consider the dual requirements of safety and economy. It is convenient to construct high polymer micro anti-slide pile for slope reinforcement, which can shorten the construction period, reduce the shaking of the slope during construction and improve the safety of the project. Safety means that the slope can maintain safety and stability after reinforcement by anti-slide pile. The

safety factor of the slope is not less than the safety factor required by the landslide treatment design, and it should not be too large to avoid waste. Therefore, the safety factor after reinforcement of the slope is taken as an optimization factor affecting the design of anti-slide pile. With the change of pile position, the thrust of landslide behind pile will also change. Smaller horizontal resistance means less engineering materials and quantities to meet the economic requirements. Therefore, the thrust of landslide behind pile is selected as an optimization factor affecting the design of anti-slide pile. In the process of anti-slide pile design, the design of pile length is also very important. If the length of the pile is small and the critical sliding surface is too deep, the expected reinforcement effect will not be achieved. If the pile is too long, the construction difficulty will increase and materials will be wasted, which will lead to local cracking of the pile (Emirler et al. 2020). The design pile length is regarded as an optimization factor affecting the design of anti-slide pile.

Because the slenderness ratio of the micro anti-slide pile is greater than 30 and the diameter is generally less than 400 mm, when the polymer slurry is used as the pile material, considering that the formed polymer micro pile is a flexible reinforced solid, excessive horizontal stress may cause damage to the pile and cause shear failure, combined with the good deformation performance of polymer material, the mises stress of pile is introduced as an optimization factor to influence the design of anti-slide pile (Khanmohammadi and Fakharian 2018). Von Mises Stress is mentioned in elastic-plastic mechanics (Mingxiang 2003) as a yield criterion whose value we usually call mises stress. In post-processing of finite element analysis software, we usually call it Mises stress, which follows the fourth strength theory of mechanics of materials. Mises stress is a kind of stress based on shear strain energy, and its value is shown in equation (1).

$$\sqrt{\frac{(a_1-a_2)^2+(a_2-a_3)^2+(a_3-a_1)^2}{2}} \tag{1}$$

Where a_1, a_2 and a_3 refer to the first, second and third principal stresses respectively. When the shape change ratio reaches a certain degree, the material begins to yield. Mises stress uses stress contour to represent the stress distribution in the model, which can clearly describe the change of a result in the whole model, so that analysts can quickly determine the most dangerous area in the model. Therefore, mises stress is selected as one of the evaluation indexes.

In this paper, safety factor, landslide thrust behind pile, pile length and mises stress are selected as the four optimization objectives which affect the design of anti-slide pile.

4 Method of multi factor comprehensive evaluation on reliability of anti-slide pile

4.1 Introduction of reliability method

In the multi-factor comprehensive evaluation method, we regard the research object as a system and make decisions according to the way of giving weight, comparative judgment and comprehensive evaluation, and it has become an important tool for system analysis after mechanism analysis and statistical analysis. The method is to combine the influence of various factors on the results, and the weight value in the multi-objective comprehensive

evaluation method will directly or indirectly affect the results, and the influence degree of each factor on the results is quantitative to make the results clear and definite. In particular, it can be used for the systematic evaluation of unstructured characteristics and multi-objective and multi criteria. Comprehensive multi factor evaluation method and characteristics of anti-slide pile design, four factors affecting the selection of design scheme: landslide thrust behind pile, pile length, mises stress and safety factor have a great influence on the final result. The relationship between them is quantified by multi-objective comprehensive evaluation method. Through simple mathematical calculation, the anti-slide pile can achieve the expected reinforcement effect within the specified time and under the specified conditions. At the same time, it also includes the safety, applicability, economy and durability of the structure. When measured by probability, the optimal reliability can be obtained and the most reasonable design scheme of anti-slide pile can be found (Li and Wei 2018).

4.2 influence of various factors

In this paper, among the four influencing factors of landslide thrust, pile length, mises stress and safety factor, the value of the safety factor is larger, the reinforcement effect of anti-slide pile is better, the value of other factors are smaller, the reinforcement effects of anti-slide pile are better. Therefore, the bigger the better formula and the smaller the better formula are introduced to evaluate the anti-slide pile design in different cases. In this method, any original value of the objective function group is mapped to the interval [0,1] through the max-min normalization through the linear transformation of the original data. S is the relative superior membership of the objective value. The bigger the better formula is as equation (2). The smaller the better formula is as equation (3). Where: α_{ij} is the target value of the target i of the jth scheme, $\alpha_{\max}$ and $\alpha_{\min}$ are the maximum and minimum values of the corresponding target respectively.

$$S_{ij} = \frac{\alpha_{ij} - \alpha_{\min}}{\alpha_{\max} - \alpha_{\min}} \tag{2}$$

$$S_{ij} = \frac{\alpha_{\max} - \alpha_{ij}}{\alpha_{\max} - \alpha_{\min}} \tag{3}$$

4.3 Multi factor comprehensive determination of reliability

The relative superior membership degree values of the target values of different schemes obtained above are synthesized, the reliability (k_j) of different anti-slide pile design schemes is determined, its value is calculated according to equation (4).

$$k_j = \frac{1}{1 + \frac{\sum_{i=1}^{4} \alpha_i \left| s_{ij} - 1 \right|^2}{\sum_{i=1}^{4} \left(\alpha_i s_{ij} \right)^2}} \tag{4}$$

4.4 Determination of weight coefficient of each factor

In this paper, four influencing factors of landslide thrust (E_1), pile length (E_2), mises stress (E_3), safety factor

(E_4) are considered. Under comprehensive consideration, combined with construction conditions, engineering experience and expert opinions, the weight coefficients of the four factors are given, as shown in Table. 2.

5 Optimal selection of design parameters of anti-slide pile

5.1 Optimal embedded depth of slope reinforced by anti-slide pile

When the anti-slide pile is used to reinforce the slope, a part of the pile needs to be driven into the embedded layer, so that the anti-slide pile can provide the anti-slide force against the sliding of the weak layer, but the deeper the pile is driven into the embedded layer, the better. When the anti-sliding piles can provide sufficient anti-sliding force, if the length of piles is increased blindly, the difficulty and the cost of construction will be increased, lead to half the battle. Therefore, the selection of reasonable embedded depth is an important part of anti-slide pile design. In the process of numerical simulation of slope reinforced by anti-slide piles, the simulation of embedded depth of 4 m, 3 m, 2 m, 1 m, 0 m and -1 m is carried out respectively, and the safety factors of different embedded depth are obtained as shown in Fig.3.

It can be seen from Fig. 3 that when the pile is not driven into the embedded layer and l_e = -1 m, the safety factor of the slope is F_s= 1.25; when there is no pile, the safety factor is F_s= 1.205. Compared with l_e = , 1, 2, 3 and 4 m, the reinforcement effect can not meet safety factor requirement when l_e = -1 m. The pile displacement diagram with embedded depth of 0-4 m can be obtained and the first row of pile displacement diagram can be used for analysis. Fig.4. shows the relationship between pile displacement and pile length, it can be seen from the diagram that the deformation degree of the pile decreases gradually from the top to the bottom, when the length of the pile reaches the depth of the embedded layer, the deformation state of the pile changes, the deformation of the pile above the embedded layer changes greatly, while the deformation of the pile below the embedded layer changes slightly. The soil resistance and friction between piles provided by the soil above the embedded layer are less than those provided by the soil below the embedded layer. The deeper the embedded depth is, the displacement of the pile top increases gradually and remains unchanged, when l_e =2, 3 and 4 m, the displacement of the pile is basically the same with the pile length. It can be found from the analysis that when l_e =2,3 and 4 m, the pile body is pushed by the soil behind the pile, the soil resistance in front of the pile, and the friction force between the pile and the soil after combining with the resistance provided by the pile body, the effect is basically the same, which makes the displacement of the pile body no longer affected by the embedded depth when l_e =2 m and larger.

Fig.5. describes the relationship between pile length and mises stress at different embedded depths. From the diagram, it can be seen that when l_e=2, 3, 4 m, the first row of piles is subjected to the maximum mises force, which is the most dangerous area in the model and is most prone to shear failure.

It can be seen that mises stress of the pile body will change with the increase of the length of the pile, firstly it increases slowly, then it accelerates to a local maximum value when it is near the embedded layer, then it decreases to a certain extent, and finally it reaches the absolute maximum value near the bottom of the pile. Through analysis,

it can be concluded that the pile in soft soil layer has great deformation. At the junction of soft soil layer and embedded layer, the stress state of pile body changes, the Poisson ratio of soil body changes and the degree of deformation changes accordingly. The upper part of pile body is easy to be deformed and the lower part is not easy to be deformed, which makes mises stress here change abruptly. It can be further concluded that the interface between soft soil layer and embedded layer and near the bottom of the pile is the most dangerous area of the pile, which is most likely to cause shear failure. Therefore, relatively small mises stress can make the anti-slide pile work better and ensure its service life and reinforcement effect. Fig.6. describes the relationship between mises stress of the most vulnerable pile and its shape length. By comparing the mises stresses of the first row of piles, it can be seen from the figure that the maximum mises stresses increase with the increase of embedded depth. The maximum mises stress is 3.21 MPa when l_e =4 m and 2.63 MPa when l_e =1 m.

With the change of pile position, the thrust force of landslide behind the pile will also change. Lower horizontal resistance means less engineering material and quantity, and also can meet the economic requirements. Fig.7. describes the relationship between the thrust of soil behind piles and the length of piles at different embedded depths. It can be seen from the diagram that the force magnitude of the first row and the fifth row of piles is larger than that of the second, third and fourth row piles. Extremum of landslide thrust of the second, third and fourth rows of piles gradually decreases. Maximum thrust of landslide on the fifth row of piles. The landslide thrust of the pile body above the embedded layer reaches the first maximum value and that of the pile body below the embedded layer reaches the minimum value. The landslide thrust of the pile body above the embedded layer reaches the first local maximum value and that of the pile body below the embedded layer reaches the local minimum value; at 2-3 m below the embedded layer, the landslide thrust on the pile body reaches the second local maximum value. At the same time, it can be concluded from the diagram that the change of embedded depth has little influence on the thrust of landslide behind the piles, but the change of embedded depth will affect the thrust of landslide shared by the middle row of piles. The greater the embedded depth, the more evenly the middle row piles are allocated, on the contrary, there will be some differences in the force of the piles.

Fig.8. describes the relationship curve between pile length and landslide thrust when pile body is subjected to maximum landslide thrust. The fifth row of piles is subjected to the greatest landslide thrust, so the landslide thrust of the fifth row of piles at different embedded depths is taken as the evaluation object. It can be seen from the diagram that when above the embedded layer, the change of the embedded depth has little influence on the force of the pile, and reaches the maximum value when about 1 m above the embedded layer. Under the embedded layer, the stress of pile increases with the increase of embedded depth, and when l_e =4 m, the stress of the pile will have a decreasing trend. This means that the selection of insertion depth of 4m is too conservative and wastes unnecessarily.

The method of comprehensive evaluation of reliability of anti-slide piles by multiple factors is used to evaluate the optimum embedded depth. The optimum selection and analysis of embedded depth is shown in Table

3.

It is calculated that the maximum reliability value is k=0.592 when l_e =2 m. The anti-slide pile is mainly used to reinforce the slope by resisting the thrust of landslide behind the pile, so the scope of landslide mass behind the pile has a vital influence on the reinforcement effect. When considering multi-row piles to reinforce slope comprehensively, the optimum embedded depth H is about 1/8-1/12 of the horizontal length of landslide mass behind piles.

5.2 Optimum pile layout location for slope reinforcement with anti-slide piles

The selection of pile location is very important for the design of micro-high polymer anti-slide piles. The same number of piles will produce very different reinforcement effects under different pile location selection. Choosing a suitable location can reduce the construction difficulty and the project cost, and more importantly, can improve the reinforcement effect of anti-slide structure. In this paper, the finite element analysis software is used to carry out numerical simulation of micro-high polymer anti-slide piles at horizontal distance from the top of the slope of p_x =0 m, 10 m, 15 m, 20 m, 22.5 m, 25 m, 27.5 m, 30 m and 35 m respectively. The safety factors of anti-slide piles, thrust force of landslide behind the pile and mises stress of the pile body at different pile positions are obtained. Fig.9. describes the relationship curve between safety factor and pile position, and Fig.10. describes the relationship curve between pile position displacement and pile length when pile position is p_1, p_2 and p_3. From Figure 9, it can be seen that when the pile position is p_1, p_2 and p_3, the safety factors are 1.271, 1.331 and 1.335 respectively, and the reinforcing effect is not ideal. Moreover, it can be seen from Figure 10 that there are certain differences in the displacement of each row of piles. Each row of piles can not work together, so it is no longer considered as the best pile position when the pile position is p_1, p_2 and p_3.

When p_x=20 m, 22.5 m, 25 m, 27.5 m, 30 m and 35 m, each row of piles can play a synergistic role. The displacement of each row of piles is basically the same, so the displacement of the fifth row of piles is taken as the evaluation object. As p_x increases gradually, the thrust of landslide behind the pile increases gradually, the resistance of soil before the pile decreases gradually, and the displacement of pile position increases accordingly. Fig.11. describes the relationship curve between the displacement of the fifth row of piles and the length of piles under different pile positions. It can be seen from the diagram that the displacement of pile position is less than p_x=27.5 m at p_x=30 m and 35 m. The reason for this phenomenon is that when p_x=30 m and 35 m, the vertical displacement of the top of the slope is too large to meet the requirements, and the horizontal displacement of the foot meets the requirements. The plastic penetration area and the horizontal displacement of the foot can not be used as the basis for judging the stability of the slope. A smaller safety factor is required. Therefore, when p_x=30 m and 35 m, the displacement of the pile body is smaller than that when p_x=27.5 m. Table 4 shows the relationship between safety factor, horizontal displacement of foot and vertical displacement of top of slope.

Safety factor is one of the key factors for evaluating anti-slide pile reinforcement of slope. At the same time,

the thrust of landslide behind pile and mises stress of pile also affect the design of anti-slide pile. Fig.12. describes the relationship curve between mises stress and pile length at different pile positions. It can be seen from the diagram that when the length of the pile reaches the depth of the embedded layer, the mises force acting on the pile body will reach an extreme value, but not the maximum value; it will reach the maximum value at the bottom of the pile. When the pile position is selected to be arranged above the middle of the slope, the mises force of the fifth row of piles is the largest among the five rows. The fourth row of piles is subjected to the maximum mises force when the pile position is selected to be arranged under the slope. The pile body is most likely to be damaged under the action of the soil pressure behind the pile and the soil resistance in front of the pile, at this time, the anti-sliding structure may not achieve the expected effect, reduce the service life of the anti-sliding structure and cause the failure of the anti-sliding structure.

Fig.13. describes the curve between mises stress of the most vulnerable pile and its length. From the diagram, it can be seen that the mises stress of the pile body has a great relationship with the choice of pile position. With the change of pile position, the fragile state of the pile body changes in the multi-row pile structure. As the position of the pile gets closer and closer to the lower part of the slope, the most easily damaged pile body gradually changes from the rear pile to the front pile, and it is not that the farther the pile position is arranged, the more likely the pile body is to be damaged. At p_x=30 m and p_x=35 m, due to the influence of excessive vertical displacement of the top of the slope, a smaller safety factor is selected so that the mises stress of the pile body is smaller at this time. When p_x=22.5 m and 25 m, the maximum mises stress of pile body is less than p_x=27.5 m and 20 m. Therefore, it is inferred that the fragile pile body changes from the front pile to the rear pile with the change of pile position from the upper part of slope to the lower part of slope, at the same time, the value of maximum mises stress changes with the change of fragile pile from rear to front. When the number of rows of fragile pile changes, the maximum mises stress changes periodically from small to large.

Fig.14. describes the relationship curve between pile length and maximum landslide thrust at different pile locations. It can be seen from the diagram that although the selection of safety factor is small at p_x=30 m and 35 m, it has little effect on the thrust of landslide behind the pile. At p_x=20 m, 22.5 m, 25 m, 27.5 m, 30 m and 35 m, the thrust of landslide behind piles changes parabolically with the position of piles from the upper part of slope to the lower part of slope, and reaches the maximum near the middle of slope.

As shown in Table 5, it is calculated that the maximum reliability value of slope reinforcement with multi-row high polymer micro anti-slide piles is k=0.483 when the location of pile laying is p_x=30 m. Therefore, the optimum position of multi-row high polymer micro anti-slide piles is 0.55-0.65L from the top of the slope, L is the horizontal distance between the top and the foot of the slope.

6 Conclusion

In this paper, the design optimization of slope reinforcement with multi-row high polymer micro anti-slide

piles is discussed, the safety factor of slope, landslide thrust behind pile, mises stress on pile and pile length are considered when anti-slide pile is embedded in different depth and pile position, based on the finite element method and multi factor comprehensive evaluation, the optimal reliability of slope reinforced by polymer micro anti-slide pile is studied. The main conclusions are as follows:

(1) With the increase of embedded depth, the safety factor of slope gradually increases and then remains stable, the mises stress of pile body gradually increases, and the vulnerability of pile body increases; the change of embedded depth has little influence on the thrust force of landslide behind pile.

(2) When using multi-row high polymer micro anti-slide piles to reinforce slope, the best embedded depth H is about 1/8-1/12 of the horizontal length of the landslide mass behind the piles, which is obtained by multi-factor comprehensive evaluation method.

(3) As the pile position is gradually away from the top of the slope, the safety factor of the slope reaches its maximum value in the middle and lower part of the slope; it is inferred that the fragile state of the pile body changes from the front pile to the rear pile; the thrust value of the landslide behind the pile changes parabolically and reaches its maximum value near the middle of the slope.

(4) When using multi-row high polymer micro anti-slide piles to reinforce the slope, the optimum position of pile arrangement is 0.55-0.65L from the top of the slope, which is obtained by multi-factor comprehensive evaluation method, L is the horizontal distance between the top and the foot of the slope.

Due to its strong adaptability, durability, fast forming speed, anhydrous reaction and small disturbance in construction process, mechanical properties are characterized by high pull-out force, high shear force and group piles synergistic forces, polymer micro anti-slide piles have broad application prospects in future slope reinforcement projects.

Acknowledgements

The work present in this paper was supported by the National Key Research and Development Program of China (2019YFC1510803); National Natural Science Foundation of China (Grant No.51639002, 51708310); China Postdoctoral Science Foundation (2019M662533); Open Research Fund of State Key Laboratory of Geomechanics and Geotechnical Engineering, Institute of Rock and Soil Mechanics, Chinese Academy of Sciences (Grant NO.Z017012). These financial supports are gratefully acknowledged.

Reference

Naudts, A. 2003. Irreversible Changes in the Grouting Industry Caused by Polyurethane Grouting: An Overview of 30 Years of Polyurethane Grouting. American Society of Civil Engineers, 519.

Wang, F.M., Guo, C.C. & Gao, Y. 2014. Formation of a Polymer Thin Wall Using the Level Set Method. International Journal of Geomechanics, **14**, 10.

Hao, M.M., Wang, F.M., Li, X.L., Zhang, B. & Zhong, Y.H. 2018. Numerical and Experimental Studies

of Diffusion Law of Grouting with Expansible Polymer. Journal of Materials in Civil Engineering, **30**.

He, C., Hu, X.L., Liu, D.Z., Xu, C., Wu, S.S., Wang, X. & Zhang, H. 2020. Model tests of the evolutionary process and failure mechanism of a pile-reinforced landslide under two different reservoir conditions. Engineering Geology, **277**, 14.

Liu, D.Z., Hu, X.L., Zhou, C., Xu, C., He, C.C., Zhang, H. & Wang, Q. 2020. Deformation mechanisms and evolution of a pile-reinforced landslide under long-term reservoir operation. Engineering Geology, **275**, 11.

Ausilio, E., Conte, E. & Dente, G. 2001. Stability analysis of slopes reinforced with piles. Computers and Geotechnics, **28**, 591-611.

Gao, Y.F., Ye, M. & Zhang, F. 2015. Three-dimensional analysis of slopes reinforced with piles. Journal of Central South University, **22**, 2322-2327.

Xue, D.M., Li, T.B., Zhang, S., Ma, C.C., Gao, M.B. & Liu, J. 2018. Failure mechanism and stabilization of a basalt rock slide with weak layers. Engineering Geology, **233**, 213-224.

Tan, Q.W., Tang, H.M., Huang, L., Li, C.D. & Kou, T. 2018. LSP methodology for determining the optimal stabilizing pile location for step-shaped soil sliding. Engineering Geology, **232**, 56-67.

Tang, L., Cong, S.Y., Xing, W.Q., Ling, X.Z., Geng, L., Nie, Z. & Gan, F.D. 2018. Finite element analysis of lateral earth pressure on sheet pile walls. Engineering Geology, **244**, 146-158.

Li, C.H., Lin, M.L. & Huang, W.C. 2019. Interaction between pile groups and thrust faults in a physical sandbox and numerical analysis. Engineering Geology, **252**, 65-77.

Mao, W.W., Liu, B., Rasouli, R., Aoyama, S. & Towhata, I. 2019. Performance of piles with different configurations subjected to slope deformation induced by seismic liquefaction. Engineering Geology, **263**, 10.

Tang, H.M., Hu, X.L., Xu, C., Li, C.D., Yong, R. & Wang, L.Q. 2014. A novel approach for determining landslide pushing force based on landslide-pile interactions. Engineering Geology, **182**, 15-24.

Won, J., You, K.H., Jeong, S. & Kim, S. 2005. Coupled effects in stability analysis of pile-slope systems. Computers and Geotechnics, **32**, 304-315.

Cai, F. & Ugai, K. 2000. Numerical Analysis of the Stability of a Slope Reinforced with Piles Soils and Foundations, **40**.

Zhao, B., Wang, Y.S., Wang, Y., Shen, T. & Zhai, Y.C. 2017. Retaining mechanism and structural

characteristics of h type anti-slide pile (hTP pile) and experience with its engineering application. Engineering Geology, **222**, 29-37.

Disfani, M., Evans, R., Gad, E., Mehdizadeh, A. & Jennings, W. 2018. PERFORMANCE OF BATTERED MINI DRIVEN PILE GROUP IN BASALTIC CLAYS: FIELD TESTING AND NUMERICAL MODELLING. Australian Geomechanics Journal, **53**, 77-87.

Surjandari, N.S., Dananjaya, R.H. & Utami, E.C. 2017. SLOPE STABILITY ANALYSIS USING MINI PILE: A CASE STUDY IN CIGEMPOL RIVER, KARAWANG, WEST JAWA. International Journal of Geomate, **13**, 49-53.

Kourkoulis, R., Gelagoti, F., Anastasopoulos, I. & Gazetas, G. 2011. Slope Stabilizing Piles and Pile-Groups: Parametric Study and Design Insights. Journal of Geotechnical and Geoenvironmental Engineering, **137**, 663-677.

Emirler, B., Tolun, M. & Yildiz, A. 2020. Investigation on determining uplift capacity and failure mechanism of the pile groups in sand. Ocean Engineering, **218**, 11.

Khanmohammadi, M. & Fakharian, K. 2018. Numerical Simulation of Soil Stress State Variations due to Mini-Pile Penetration in Clay. International Journal of Civil Engineering, **16**, 409-419.

Mingxiang, C. 2003. Elastic-plastic mechanics, Science Press. (in chinese)

Li, M.M. & Wei, H.W. 2018. Optimization design of pile location on slope based on multi-objective comprehensive evaluation method. Journal of Railway Science and Engineering, **15**, 1445-1452. (in chinese)

Table.1. Calculation of Model Material Parameters

material	deformation modulus E/MPa	internal friction angle φ/°	unit weight $\gamma/kN/m^3$	poisson ratio v	cohesion c/kPa
Polymer micro anti-slide pile	5000		1.46	0.35	
silty clay	10	10	2.0	0.4	30
granite	20	23	2.0	0.3	36
Polymeric soil	200	30	2.5	0.28	300

Table.2. Relative weight assignment of each target

optimization object	E_1	E_2	E_3	E_4	weight
E_1	1	1	2	1	0.25
E_2	0.5	0.5	0.5	0.5	0.1
E_3	1	1	2	1	0.25
E_4	2	2	2	2	0.4

Table.3. Optimization Analysis of Embedded Depth Selection

embedded depth	E_1/ (kN)	S_1	E_2/ (m)	S_2	E_3/ (Pa)	S_3	E_4	S_4	k
1 m	646	1	14.5	1	2626	1	1.38	0	0.527
2 m	658	0.6	15.5	0.33	2792	0.71	1.406	0.84	0.592
3 m	669	0.23	16.5	0.66	2941	0.46	1.41	0.97	0.424
4 m	676	0	17.5	0	3204	0	1.411	1	0.211

Table.4. Safety factor evaluation

	Horizontal displacement of slope toe(m)	Vertical displacement of slope top(m)	factor of safety
p_x=30 m	-0.0264	-0.1565	1.379
	-0.0310	-0.2337	1.399
	-0.0543	-0.3399	1.423
	-0.0821	-0.7183	1.443
p_x=35 m	-0.0178	-0.0955	1.360
	-0.0257	-0.1663	1.379

	-0.0401	-0.2955	1.403
	-0.064	-0.7578	1.427

386 **Table.5.** Optimization Analysis of Pile Position Selection

pile position	E_1/ (kN)	S_1	E_2/ (m)	S_2	E_3/ (Pa)	S_3	E_4	S_4	k
p_x=20 m	544	0.92	17.5	0	4779	0.05	1.362	0	0.007
p_x=22.5 m	586	0.68	16.5	0.17	3147	0.72	1.38	0.30	0.197
p_x=25 m	658	0.28	15.5	0.33	2941	0.81	1.406	0.72	0.377
p_x=27.5 m	708	0	14.5	0.5	4893	0	1.42	0.95	0.218
p_x=30 m	641	0.37	13.5	0.67	3889	0.41	1.423	1	0.483
p_x=35 m	529	1	11.5	1	2468	1	1.403	0.67	0.467

387

Figures

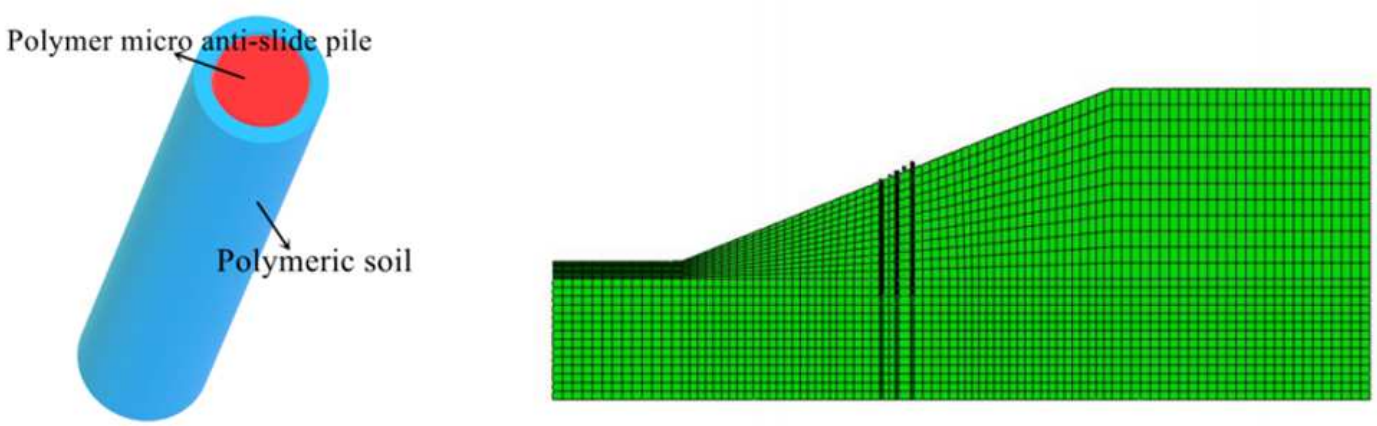

Figure 1

Polymer micro pile model and slope grid division diagram

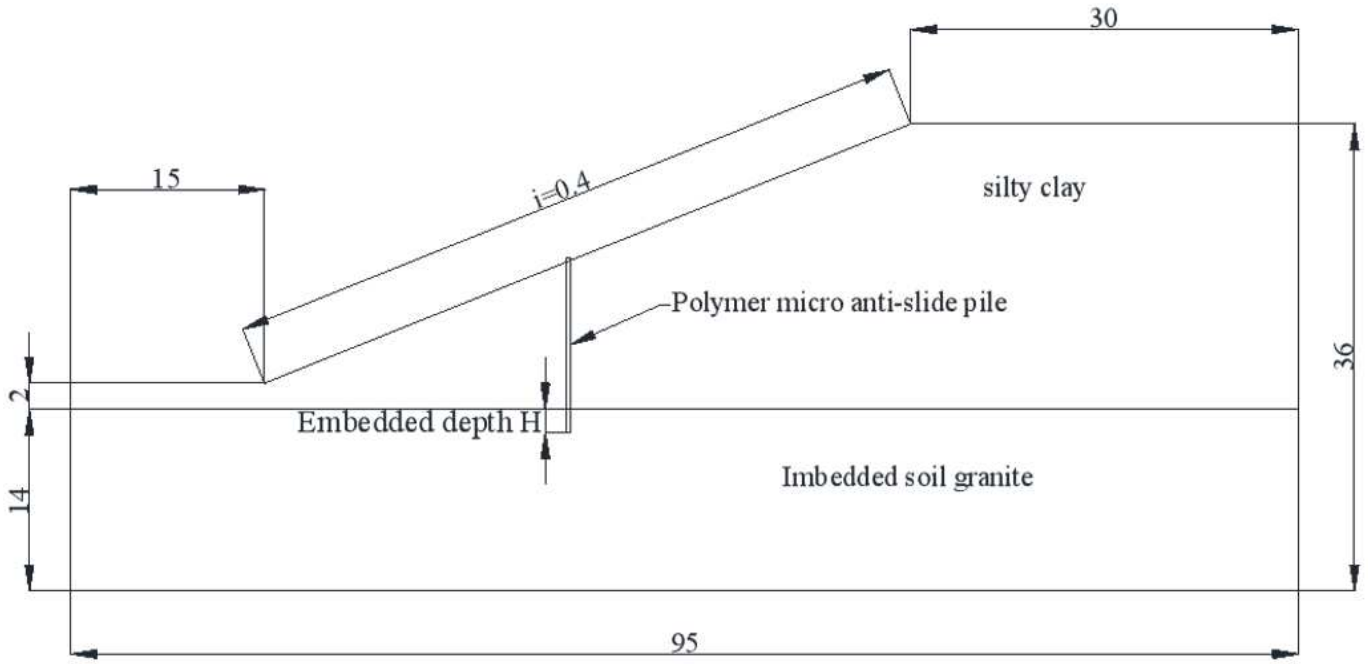

Figure 2

Slope reinforcement model with polymer micro-pile

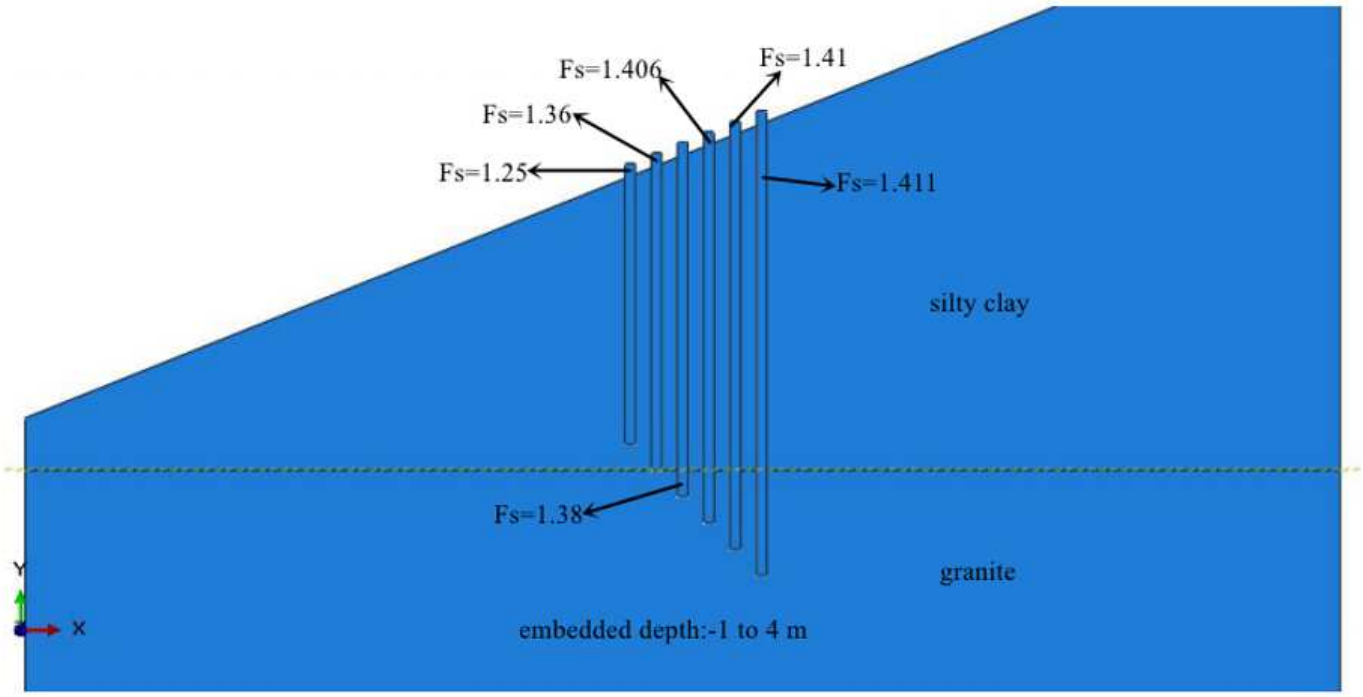

Figure 3

Safety factor at different embedded depth

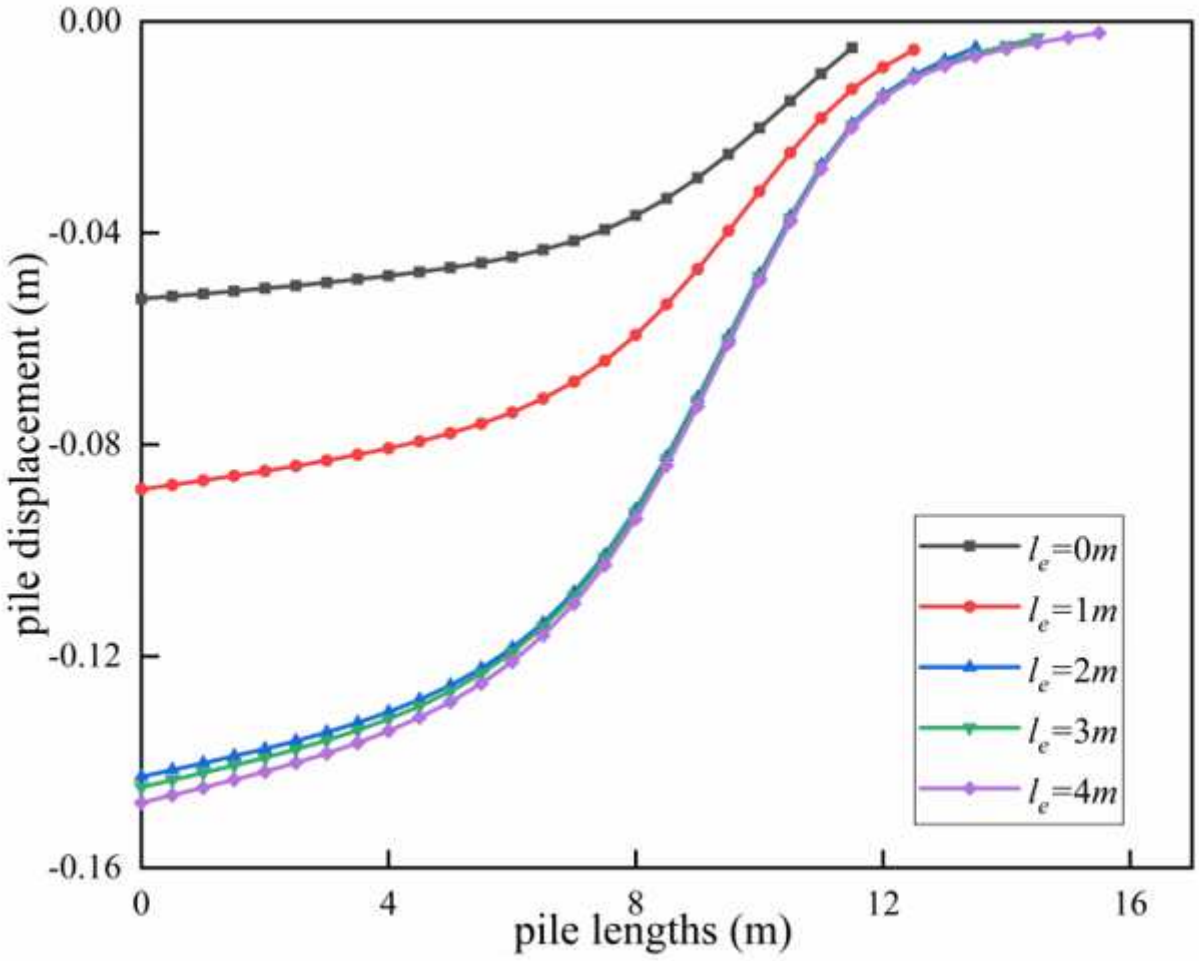

Figure 4

Pile displacement

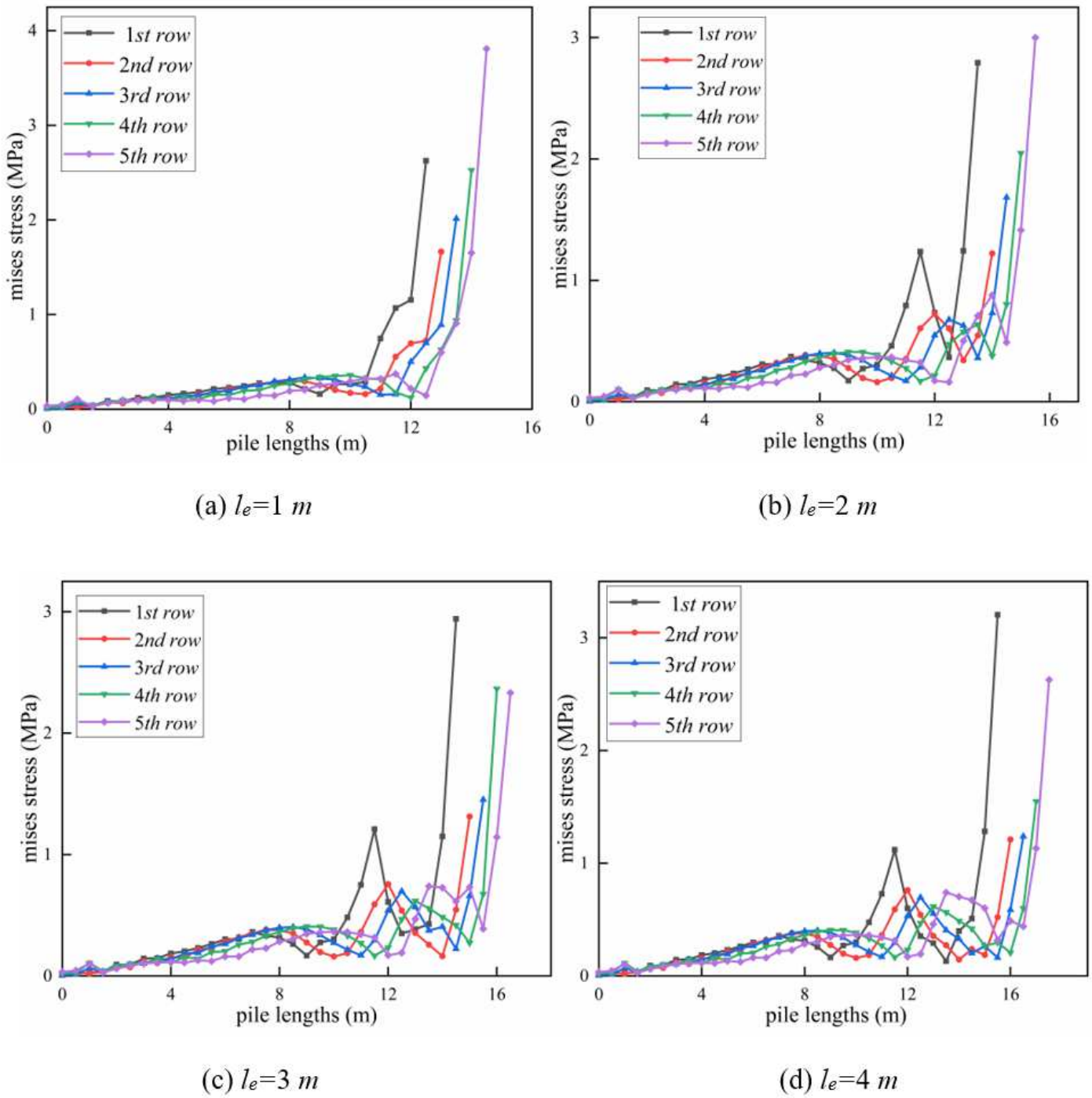

Figure 5

Mises stress of different embedded depth

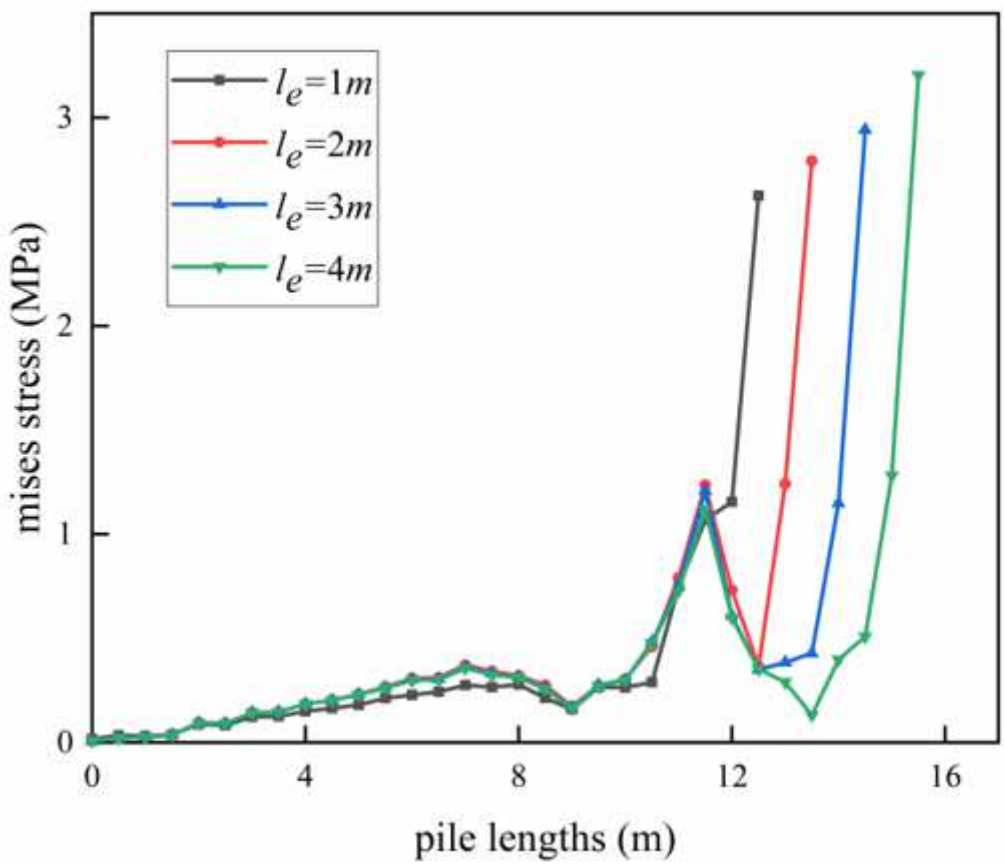

Figure 6

Mises stress of the first row piles

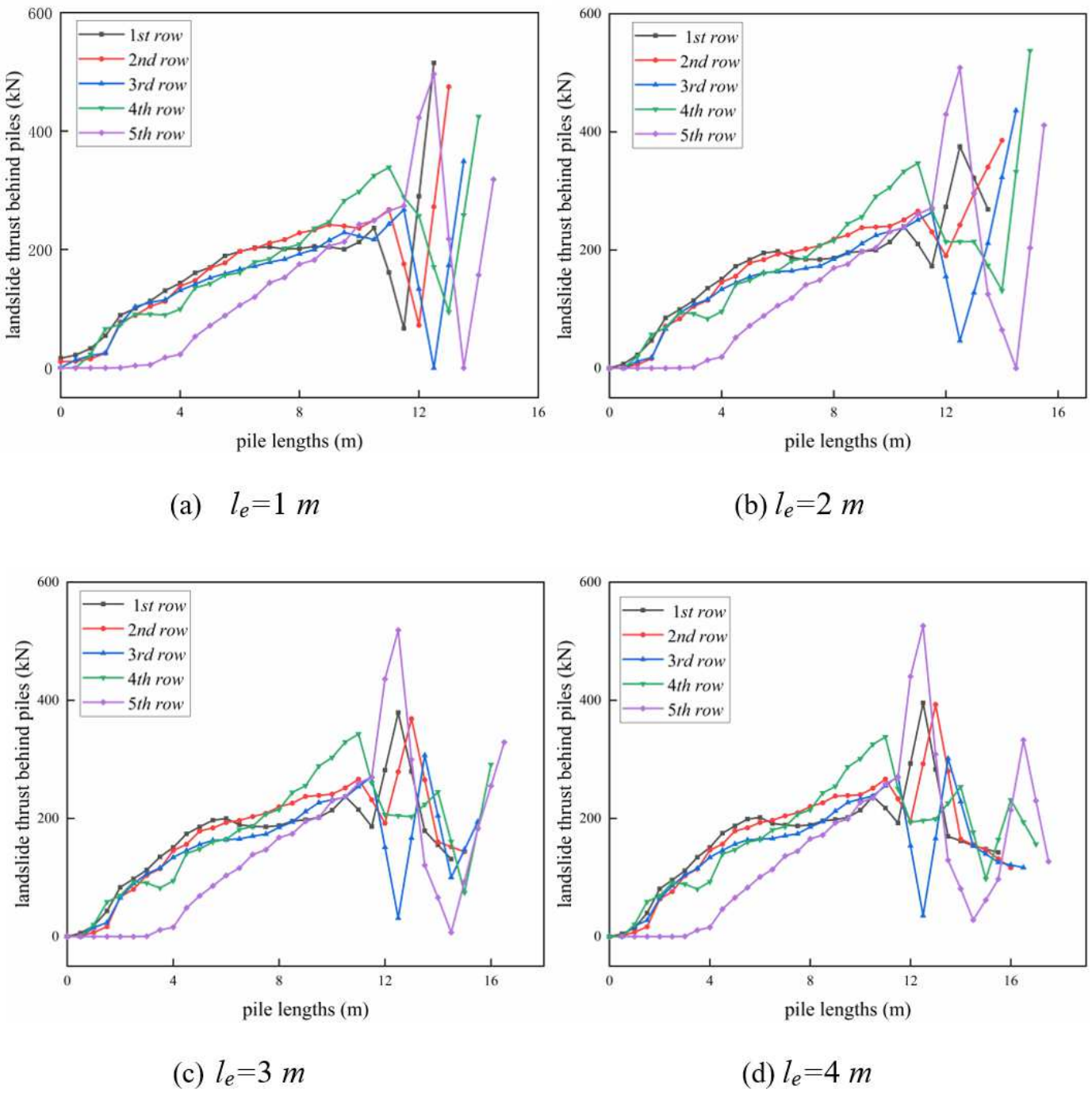

Figure 7

Landslide thrust behind piles

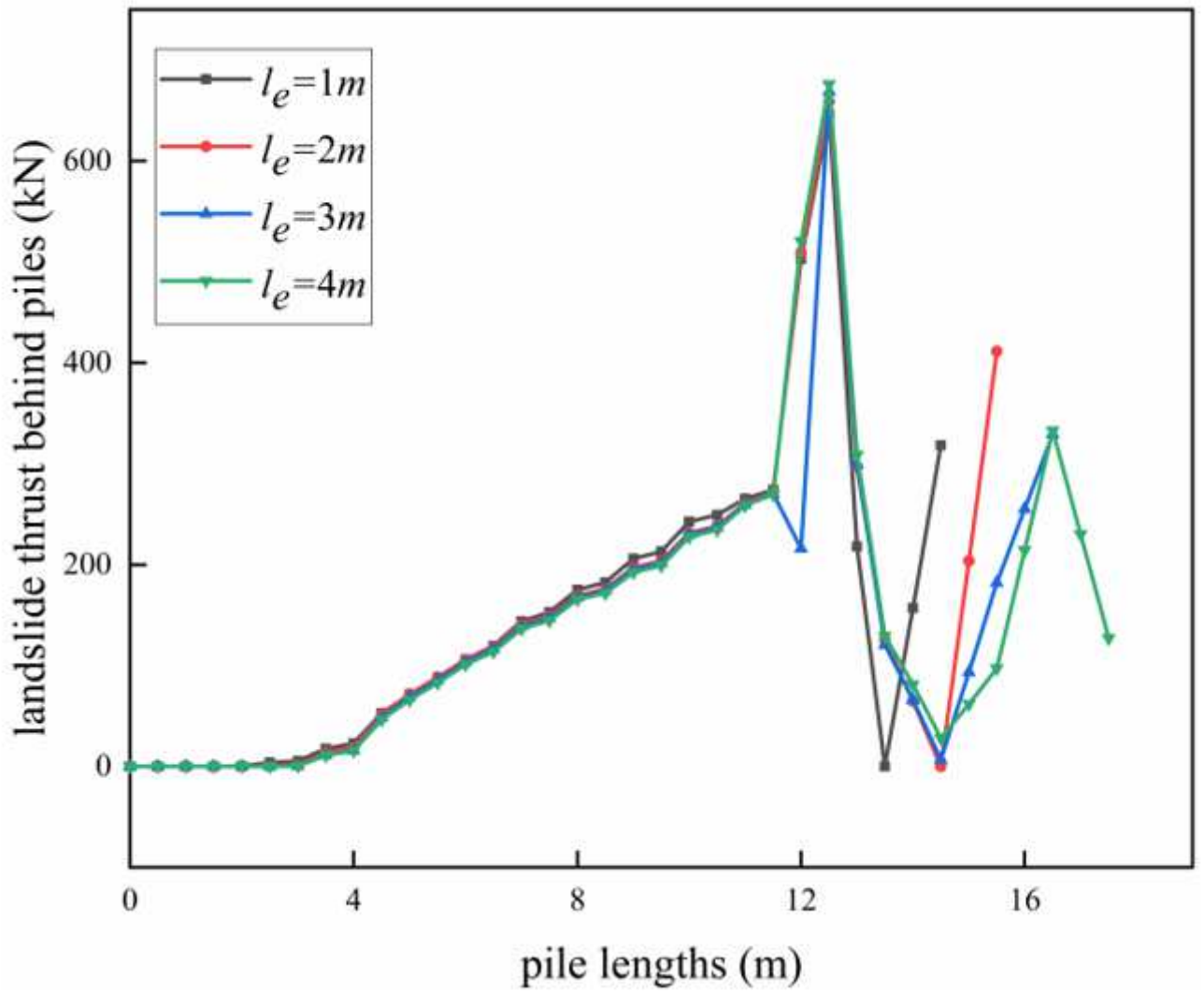

Figure 8

Thrust of landslide behind the fifth row pile

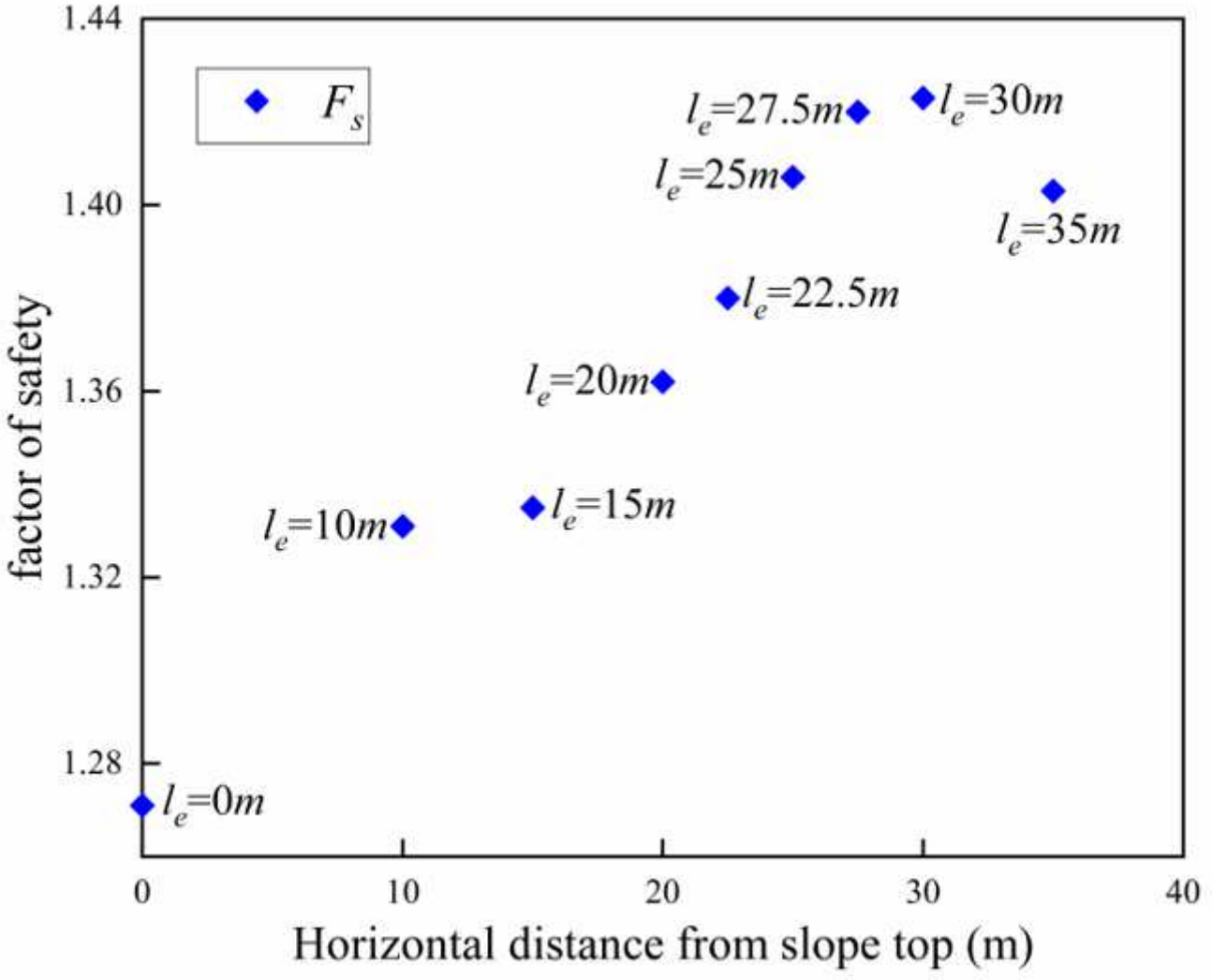

Figure 9

Safety factor diagram at different pile positions

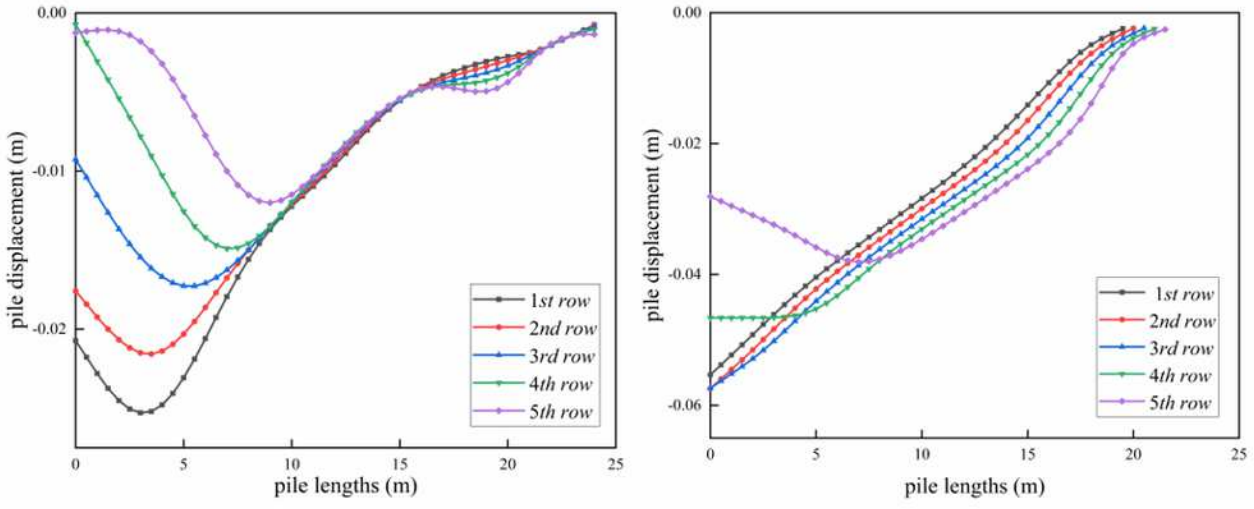

(a) p_x=0 m (b) p_x=10 m

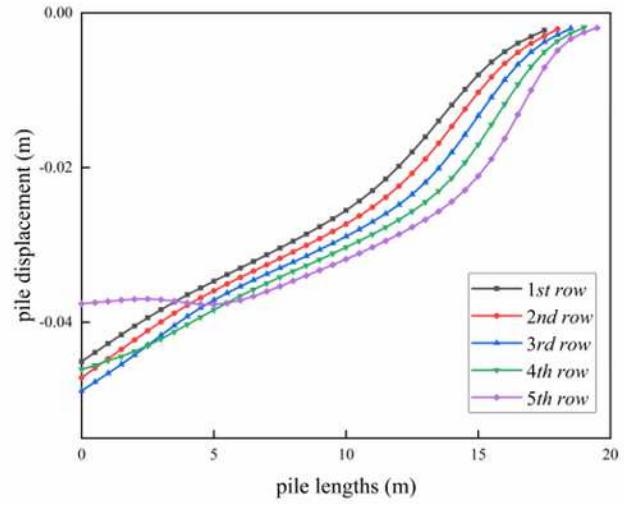

(c) p_x=15 m

Figure 10

Pile displacement at different pile positions

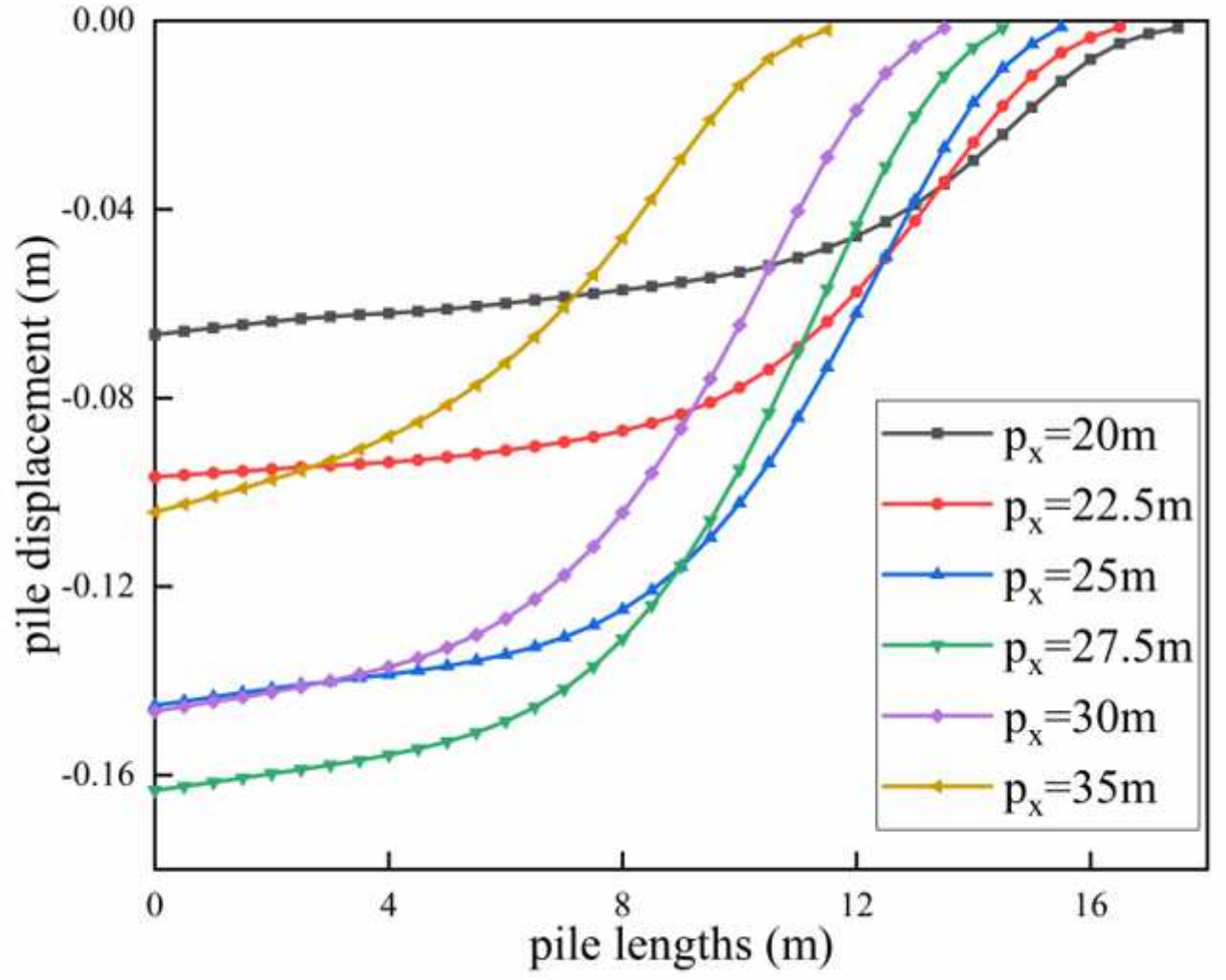

Figure 11

Pile displacement maps at different pile positions

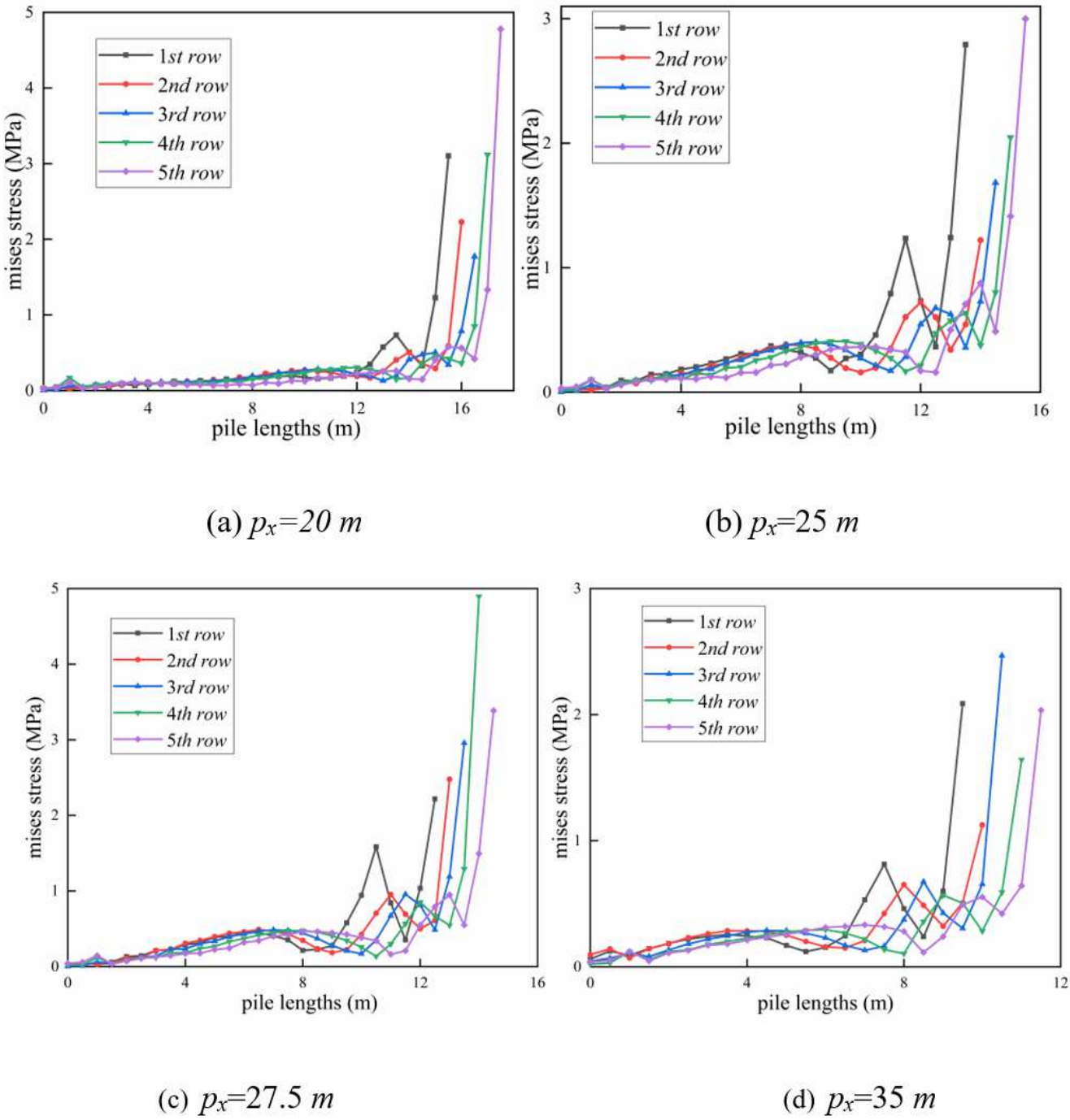

Figure 12

Mises stress at different pile positions

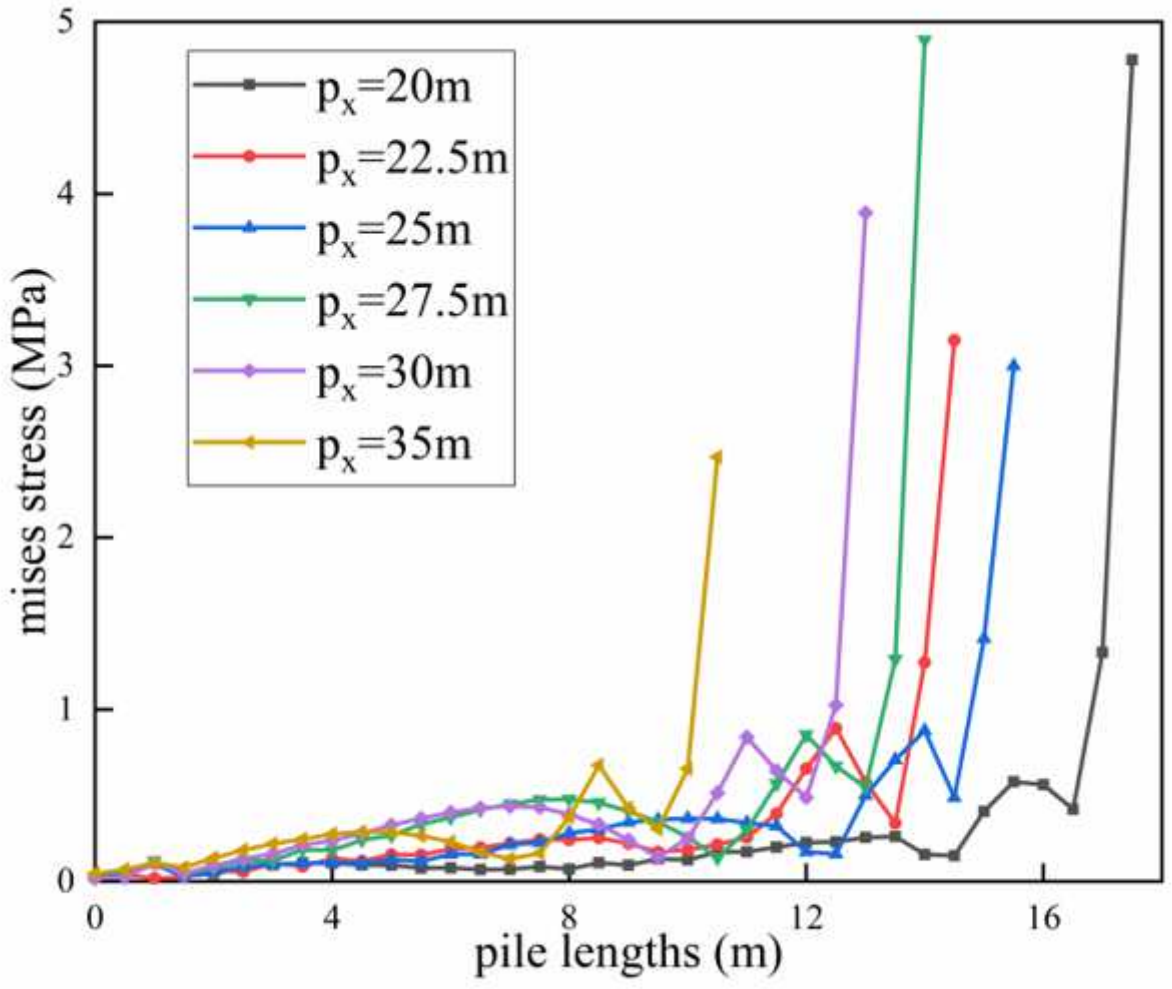

Figure 13

Maximum mises stress at different pile positions

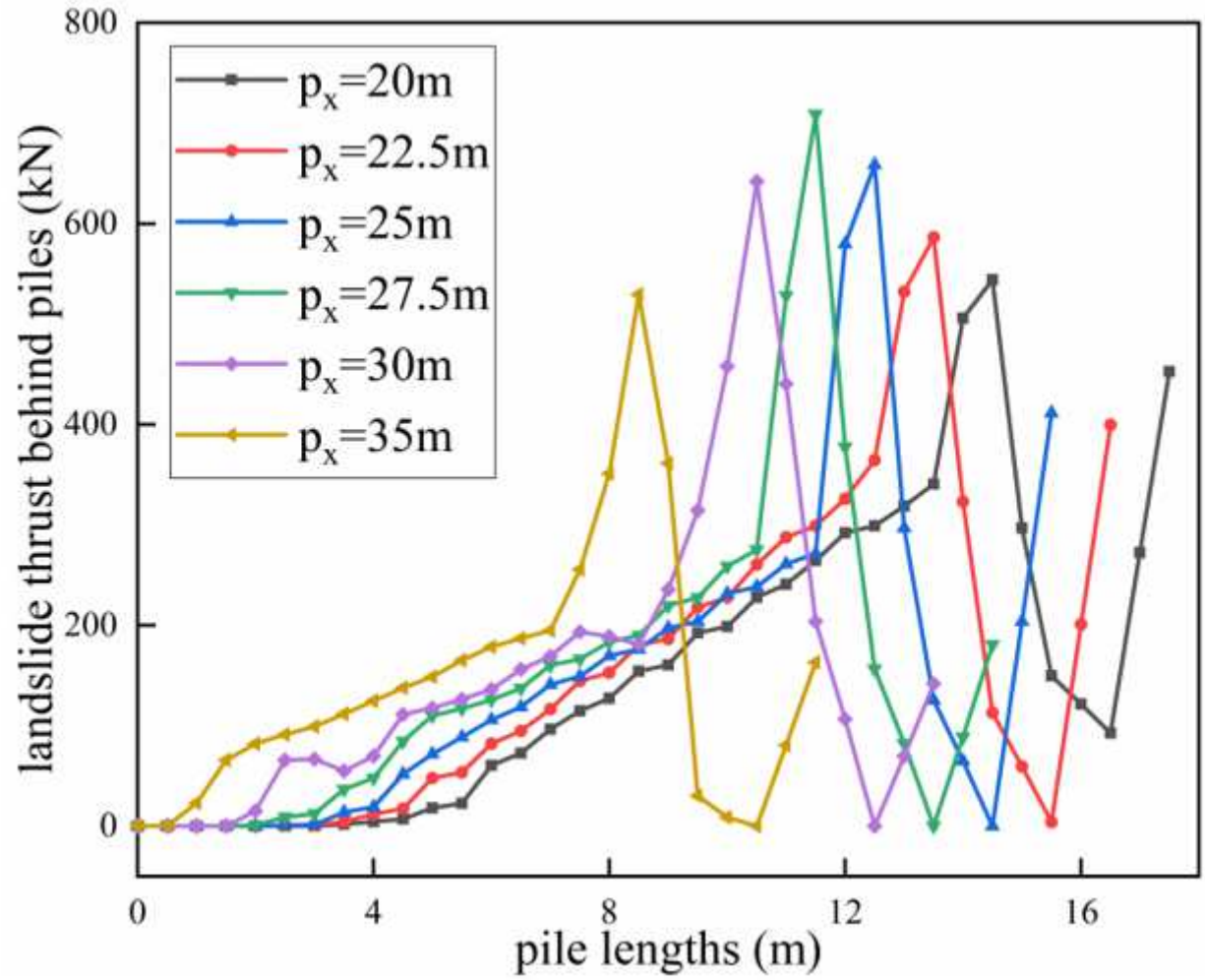

Figure 14

The thrust of landslide behind piles at different pile positions